GSI

GSI - 81 - 36
PREPRINT

ISOTOPE IDENTIFICATION IN THE TRANSFERMIUM REGION BY α-α KORRELATION AFTER IN-FLIGHT-SEPARATION

G. MÜNZENBERG, P. ARMBRUSTER, W. FAUST, K. GÜTTNER, F.P. HESSBERGER, S. HOFMANN, W. REISDORF, C.C. SAHM, K.-H. SCHMIDT, H.J. SCHÖTT, B. THUMA AND D. VERMEULEN

Contribution to 'Actinides - 1981', Asilomar, September 10-15, 1981

OKTOBER 1981

Gesellschaft für Schwerionenforschung mbH
Planckstr. 1 · Postfach 110541 · D-6100 Darmstadt 11 · Germany

ISOTOPE IDENTIFICATION IN THE TRANSFERMIUM REGION BY α-α CORRELATION AFTER IN-FLIGHT-SEPARATION

G. Münzenberg*, P. Armbruster*, W. Faust*, K. Güttner**,
F.P. Heßberger*, S. Hofmann*, W. Reisdorf*, C.C. Sahm***,
K.-H. Schmidt*, H.J. Schött*, B. Thuma**
and D. Vermeulen***

*Gesellschaft für Schwerionenforschung mbH,
Darmstadt, Germany

**II. Physikalisches Institut Universität Giessen,
Giessen, Germany

***Institut für Kernphysik, Technische Hochschule Darmstadt,
Darmstadt, Germany

ABSTRACT

Experimental results on the production of the elements Fm to 107 in heavy ion fusion reactions of ^{40}Ar, ^{50}Ti, or ^{54}Cr with isotopes of Pb or Bi are presented. The fusion products were separated from the projectile beam in-flight with their full energy as they recoil from the target. For identification they were implanted into an array of position sensitive surface barrier detectors, where α-decay or spontaneous fission were measured.

This new experimental method permitting the identification of unknown α-emitters by genetic relationship has been extended to the heaviest nuclei. The analysis of single decay chains starting from individual implanted nuclei allows to identify unknown isotopes with formation cross sections down to the 100 pb region and lifetimes down to 10^{-6} s.

All previously reported deexcitation channels for the fusion of ^{40}Ar and ^{208}Pb characterized either by spontaneous fission or by α-decay were observed for the first time in one experiment. We investigated the isotope $^{256}104$, which is important for spontaneous fission halflife systematics of the transactinides. The possibility to form cold compound nuclei close to the fusion barrier is discussed in the view of our recent experiments with respect to the fusion of ^{48}Ca and ^{248}Cm.

We report the first identification of element 107 by genetic relationship.

KEYWORDS

Heavy ion fusion, velocity filter, position sensitive surface barrier detector, genetic relationship; identification, element 107; new isotopes ^{239}Cf, ^{243}Fm, ^{247}Md, ^{253}Lr, ^{254}Lr, $^{258}105$, $^{262}107$; halflife $^{256}104$; fusion barrier.

INTRODUCTION

The investigation of the heaviest nuclei in the region of fermium and beyond does not only require more and more sensitive detection methods to identify isotopes with production cross-sections of 10^{-33} cm^2 and below but also demands the extension of the range of halflives to be investigated to regions far below seconds.

The well established techniques used so far for the identification of short lived nuclei with Z ≥ 100 from heavy ion fusion reactions, as the He-jet, rotating drums, or moving tapes have been developed to a high state of art and, hence, approached the limits of their possibilities. Their main restrictions are due to the fact that the nuclei to identifiy have to be stopped in the gasflow or solid material before they are moved to the detector positions. Isotopes with short halflives can only be detected to a limit of some tenths of seconds with the He-jet or some parts of milliseconds with the rotating drum, the latter one being only applicable to reaction products undergoing spontaneous fission.

Due to momentum transfer from the projectiles the evaporation residues formed by heavy ion fusion reactions leave the thin target with a well defined velocity. In the stopping process useful information from reaction kinematics are lost. Hence, in-flight separation seems the most suitable method to separate evaporation residues from the projectile beam or other nuclear reaction products, especially for the short lived nuclei far from stability.

With a velocity filter, separation times of 10^{-6} s and high background suppression, combined with a high efficiency for evaporation residues, are possible. The separated nuclei are implanted into position sensitive surface barrier detectors with their full recoil energy. They are identified by their α-decay or spontaneous fission.

We also have developed this experimental technique for the last five years at the velocity filter SHIP for the investigation of the heaviest nuclei.

The possibilities of the rotating drum, He-jet, and velocity filter are compared in Table 1.

TABLE 1 Main Characteristics of Different Approaches to Detect the Heaviest Nuclei with Z ≥ 104

	Rotating Drum	He-Jet	Velocity Filter
Efficiency	50 %	30 %	20 %
Separation Time	10^{-3} s	0.1 s	10^{-6} s
Efficiency Reaction Dependent	no	no	yes
Lowest Cross Section	0.1 nb	0.2 nb	0.2 nb
Detectable Decay Mode	sf	α,sf	α,sf
Genetic Relationship	no	yes	yes
Detection of Evaporation Residue	no	no	yes

KINEMATIC SEPARATION

Velocity Separation of Evaporation Residues

The fusion process is an inelastic collision between target and projectile, the velocity of the compound nucleus is then

$$V_c = V_p M_p / M_c \qquad (1)$$

M_c is the mass of the compound nucleus, M_p, V_p are mass and velocity of the projectile. The momentum of the projectile being conserved in the reaction, velocity separation equals a mass separation of fusion products. The evaporation residues, which have survived the cooling down process of the heated compound system, in case of isotropic particle evaporation have the same average velocity as the compound nuclei. In the evaporation process and by scattering in the target velocity and angular distributions are spread.

Reaction products from other binary reactions, as fusion-fission or nucleon transfer cannot move in forward direction with the velocity of the evaporation residues : The fragments are driven apart by Coulomb force, when they separate after interaction. Hence, they cannot move with center-of-mass velocity like the evaporation residues. Coulomb potential at the point, where nuclear interaction ceases, gives their minimum relative velocity. For two fragments in the exit channel the minimum center-of-mass velocity in beam direction, normalized to the velocity of the evaporation residues is given in Fig. 1 for the reaction ^{54}Cr on ^{209}Bi. Target-like transfer products have roughly double the velocity of the evaporation residues, fission products at least the threefold velocity. Even the evaporation of one α-particle gives a velocity change of about 8 % for the residue. The calculated suppression factors for given velocity deviations are also given.

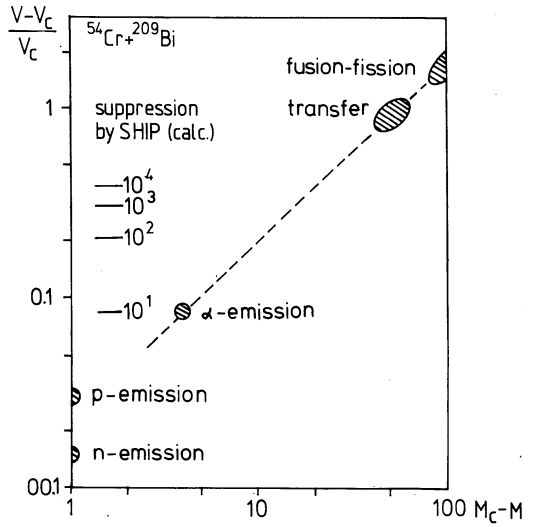

Fig. 1. Normalized center of mass velocity $(V-V_c)/V_c$ of evaporation residues (for α, p, n-emission) and heavy fragments with Mass M, vs. mass of light fragment, which is $M-M_c$. Light fragment is emitted in backward direction.

The Velocity Filter SHIP

SHIP, Fig. 2, principally operates like the Wien velocity filter, however, it has spatially separated electric and magnetic fields (Münzenberg, 1979,1981a). For efficient suppression of background from scattered projectiles or products from other nuclear reactions than fusion, SHIP has two filter stages. Each stage consists of an electric deflection condenser and two dipole magnets to generate a charge independent velocity dispersion and a quadrupole triplet for focussing. They focus the evaporation residues onto the velocity slit and the detector position, respectively. The selected velocity range is determined by a variable velocity slit behind the first stage, it is normally ± 5 %. The reaction products have highly excited electron shells and consequently cover a wide range of charge states, SHIP accepts a maximum of ± 10 %. A thin carbon foil 8 cm downstream the target equilibrates the charge distribution 20 ns after formation of the evaporation residue to avoid losses due to exotic charge states from converted transitions. The solid angle of acceptance is 2.7 msr, separation time for the reaction products is 2 µs.

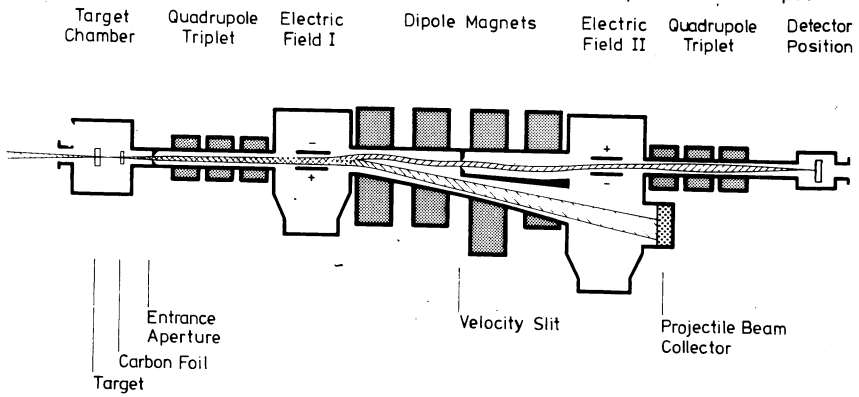

Fig. 2. The velocity filter SHIP (total length 11 m).

The efficiency is calculated with a Monte Carlo program including the recoil from evaporated neutrons, energy loss, and scattering in the target, the ionic charge distribution of the evaporation residues and the ion optical properties of SHIP (Faust, 1979). It is (15 - 30) % for the discussed reactions and increases with projectile mass. The accuracy of these calculations is estimated to be within a factor of two (Münzenberg, 1981b).

IDENTIFICATION TECHNIQUE

SHIP is designed to transport the whole group of evaporation residues originating from different deexcitation channels of the same compound nucleus. To identify a certain isotope, special detector systems are needed. For α-emitters and nuclei undergoing spontaneous fission, implantation into a surface barrier detector and measuring the decay properties of the implanted nuclei is the most suitable identification method. Fig. 3 shows an energy spectrum for ^{40}Ar on ^{144}Sm taken with a Silicon surface barrier detector at the exit of SHIP.

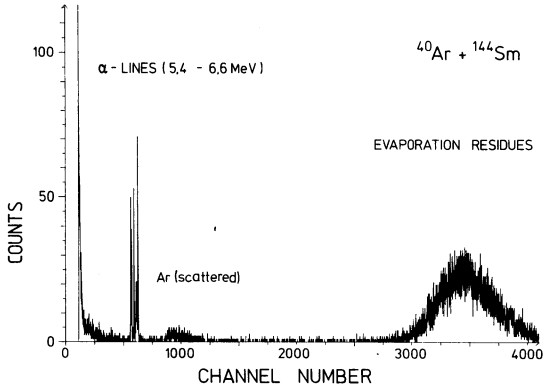

Fig. 3. Energy spectrum taken at the exit of SHIP for ^{40}Ar on ^{144}Sm.

This spectrum shows a strong peak of evaporation residues, the lines from their α-decay, and also a small peak of scattered Ar projectiles. Time-of-flight measurements show that the scattered particles have the same average velocity as the evaporation residues, which is expected for a velocity filter. Consequently, the relation between the energies of evaporation residues and scattered projectiles correspond to their masses. Sources for scattering are target frames, diaphragms, and also target inhomogeneities. In the reported experiments, the suppression of scattered projectiles is 10^{10}-10^{12}. Projectiles with original energy were rejected by more than 16 orders of magnitude.

Implantation depth for evaporation residues is (3 - 6) μm and small compared to the 60 μm range of the α-particles from their decay. Therefore, half of the α-particles escape the detector and the response is 50 %. Efficiency for spontaneous fission is 100 %, as at least one fragment is stopped in the active detector region.

The low background in the α-spectra is completely eliminated by gating between the UNILAC beam bursts, which have a length of 5 ms and are followed by 15 ms intervals (macro structure).

Position and Time Correlation

Unambiguous identification of new α-emitting isotopes is best performed in establishing decay chains leading to known transitions. A technique of position and time correlation measurements between subsequent decay signals was developed. The main point of the method described here is that for any incident nucleus, its subsequent chain of alpha decays must be observed at its position of implantation within the limits of the resolution of the detector (Hofmann, 1979,1981a,b). Such correlations can easily be determined from two dimensional plots of parent energies on the ordinate and of daughter energies, following within a certain time window and a position window relative to the parent position, on the abscissa. An example of such a plot is shown in Fig. 4.

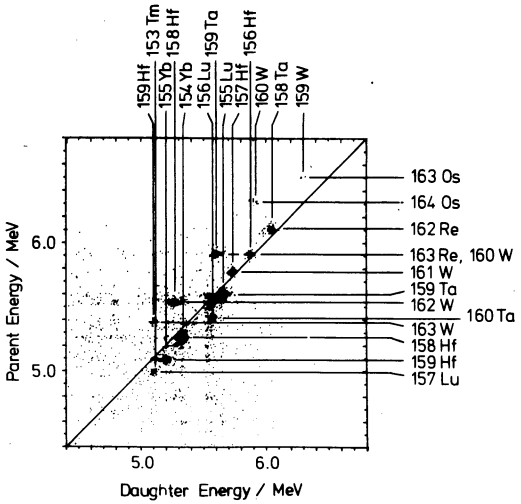

Fig. 4. α-α coincidence spectrum for ^{58}Ni on ^{110}Cd. Excitation energy of the compound nucleus ^{168}Os is 83 MeV; Time window : 200 ms; Position window : ± 0.45 mm. The plot shows 10 new isotopes.

True correlations can be found easily by an accumulation of events. Analyzing projected spectra onto the energy axis obtained with additional energy windows, positions, and intensities of correlated events can be measured very accurately even in cases of unresolved lines in complicated singles spectra. Maximum correlation time is limited by random events, e.g. evaporation residues per time and detector area.

For good efficiency we use an array of seven position sensitive surface barrier detectors with a total area of 2000 mm^2. Figure 5 shows a two-dimensional plot of the spatial distributions of α-decays from a certain

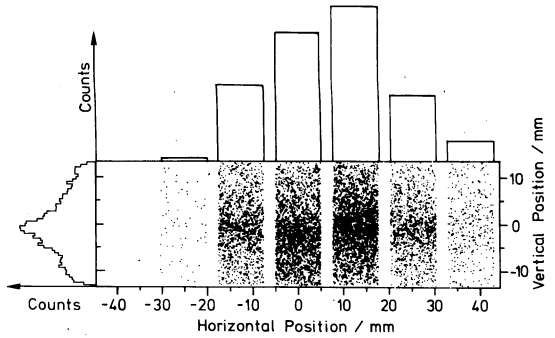

Fig. 5. Intensity distribution of ^{162}W α-decays across the detector array (horizontal distribution for each detector artificial).

evaporation residue. The detectors are position sensitive in vertical direction. Horizontal position is given by the detector number, the horizontal distribution across each detector is smeared out artificially for better presentation. The active detector area is reduced by the frames of the single detectors to 75 %. SHIP is operated with velocity dispersion in the detector plane, so the detector number corresponds to particle velocity. Ions with average velocity will be implanted in the central detector. The projections of horizontal and vertical distributions of the evaporation residues are also plotted.

Cooling the detector to 255 K, an energy resolution of 25 keV FWHM is obtained. The position resolution of 1 % gives an improvement of a factor of at least 60 for maximum correlation time.

Evaluation of Halflives

The problem of halflife evaluation for few events has been solved by use of the maximum likelihood method. The time intervals between subsequent events are plotted in logarithmic time bins. This distribution has a maximum at the average lifetime of the isotope (Schmidt, 1979). Figure 6 shows an example for the time correlation (without position conditions) as used to identify the new isotope ^{212}Th by correlation to the daughter decay of ^{208}Ra (Vermeulen, 1980).

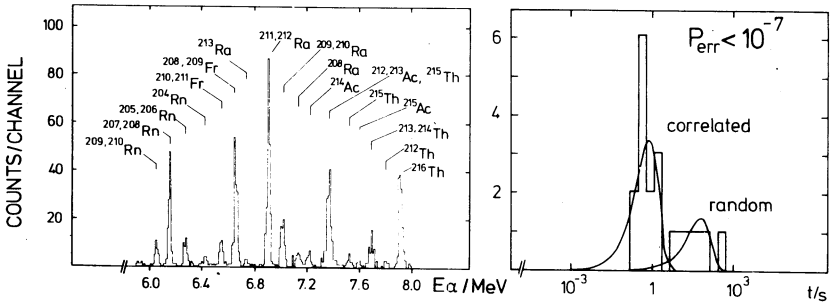

Fig. 6. Left : α-decay spectrum for ^{40}Ar (179 MeV) on ^{179}Hf.
Right: Correlation analysis between ^{212}Th and daughter α-decays. Time scale logarithmic, solid lines : Fitted time spectra for α-decays and random events. Statistical error of correlation $< 10^{-7}$.

One major advantage of the implantation technique is, that the nuclei impinging the detector give an energy, position, and timing signal. So the mother halflife can be measured without using choppers. Long lived background can be eliminated in the α-spectra as well as for spontaneous fission.

Experimental Conditions for Ar, Ti, Cr on Pb or Bi Irradiations

A schematic graph of our setup is shown in Fig. 7. Monoisotopic targets of ^{206,207,208}Pb or ^{209}Bi were irradiated with ^{40}Ar, ^{50}Ti, or ^{54}Cr. Average beam intensities were (0.5 - 1) x 10^{12} sec^{-1}, target thickness around 0.7 mg/cm^2. The specific projectile energies were close to fusion barrier and about 4.85 MeV/u

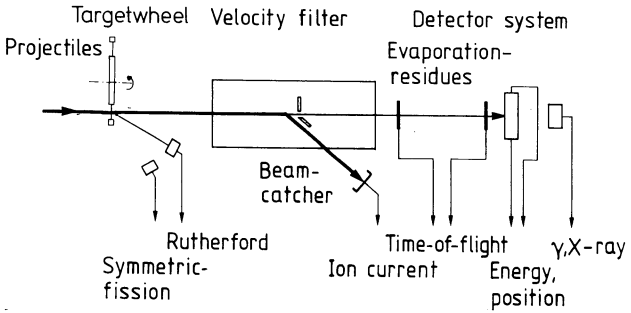

Fig. 7. Setup for ^{50}Ti and ^{54}Cr irradiations.

To withstand high beam intensities the targets were covered with carbon films of 0.03 mg/cm^2 and mounted on a wheel, which rotates synchronously to the accelerator pulsing. During subsequent beam bursts eight consecutive targets are moved across the beam axis, with a velocity of 1 cm/ms. Target thickness is monitored by Rutherford scattering.

Symmetric fission of the compound nuclei can be detected with a simple time-of-flight energy measurement in our target chamber. We used the micro-bunches of the UNILAC beam of less than 1 ns width for timing and a surface barrier detector for energy measurement (Sahm, 1980).

The separated evaporation residues pass a large area time-of-flight detector before they are implanted into the array of position sensitive detectors. From flight-time and energy of the incoming ions a rough mass estimation is possible. By an anticoincidence between time-of-flight and the surface barrier detectors, decays in the detector can be discriminated from incoming particles. The system is completed by a γ-x-ray detector. The time-of-flight detector was only disposable in the ^{50}Ti and ^{54}Cr irradiations.

EXPERIMENTAL RESULTS

A survey on reactions and isotopes investigated in the course of our experiments is given in Fig. 8. The contour line gives the known isotopes according to Lederer tables (1978). Dark squares mark the new isotopes, others observed at SHIP are indicated as bright squares.

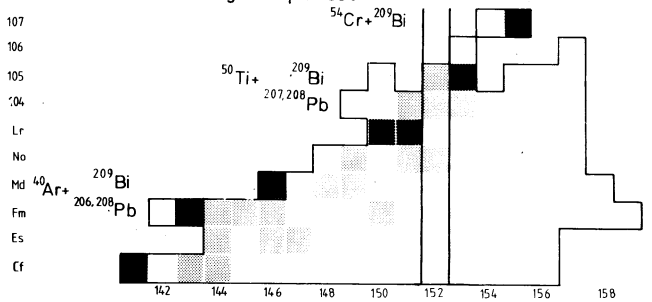

Fig. 8. Bright squares, isotopes observed at SHIP, dark squares, new isotopes. Framed area : Isotopes given in Lederer tables.

^{40}Ar and ^{50}Ti on Pb Irradiations - Neutron Deficient Fm Isotopes

The investigation of Fm isotopes from fusion of Ar and Pb is a good start to enter the region of the heaviest elements. Targets near the double magic ^{208}Pb permit the production of cold compound systems, formation cross sections are in the nanobarn region, the dominating decay modes are α-decay or spontaneous fission, and halflives range from ms to s. These are the experimental conditions also expected for the heavier nuclei.

Moreover, special deexcitation channels have been investigated carefully by various authors : ^{208}Pb (^{40}Ar, 3n) ^{245}Fm (Nitschke, 1979), and ^{206}Pb (^{40}Ar, 2n) ^{244}Fm (Gäggeler, 1979).

With our experimental setup, observation of all deexcitation channels is possible for the first time. In ^{208}Pb irradiations the isotopes ^{246},^{245}Fm were identified by their α-decay energies, halflives, and by correlations to daughter decays, the spontaneous fissioning ^{244}Fm by its halflife. In this experiment the finding of the 2n deexcitation channel by Oganessian (1975a), who only observed the spontaneous fission of ^{246}Fm, was confirmed (Münzenberg, 1981b), and also his suggestion to obtain cold heavy compound nuclei from fusion reactions with targets around the double magic ^{208}Pb. We will follow this method also for the synthesis of heavier systems.

Irradiating ^{206}Pb with ^{40}Ar we found the new isotope ^{243}Fm. Figure 9 shows an α-spectrum without correlation conditions but taken between the UNILAC beam bursts, irradiation time was 20 h, projectile dose 8 x 10^{16}. The spectrum shows the α-decay assigned to ^{243}Fm and the daughter decays of ^{239}Cf which could also be correlated. The measured cross section for ^{243}Fm production is $(1.3^{+0.9}_{-0.7})$ nb.

The spectrum also shows α-decays from transfer products. Comparison of our data for the ^{208}Pb irradiations to those of Nitschke shows that transfer products are suppressed by SHIP more than three orders of magnitude. Time-of-flight measurements show that they have the same velocity as the evaporation residues. This only can be explained by scattering processes.

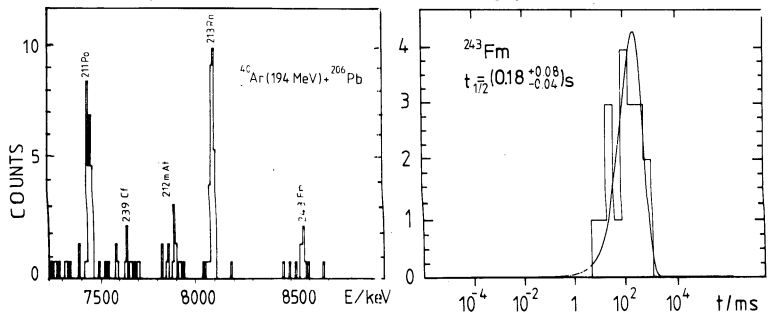

Fig. 9. α-spectrum and time correlation between implantation of the evaporation residue and subsequent α-decay for ^{40}Ar (194 MeV) on ^{206}Pb to produce ^{243}Fm.

Our cross sections, which are strongly influenced by the efficiency calculations, agree to experimental data from Gäggeler, Nitschke, and Oganessian within the error bars and indicate the reliability of our calculations, even for the region of the heaviest nuclei, where most of the parameters necessary for the ion optical calculation are extrapolated.

Figure 9 also shows the logarithmically scaled distribution of time distances between implantation and α-decay of ^{243}Fm. The solid line is the fitted distribution from which halflife has been taken.

Spontaneous fission halflife of ^{256}104. One interesting aspect to investigate element 104 is the systematics of spontaneous fission halflives for even-even nuclei, which changes abruptly between No and element 104 according to experiments of Oganessian (1975b). The enhancement of halflives on the N = 152 subshell disappears. For the isotope ^{256}104 the effect is about four orders of magnitude (Fig. 10).

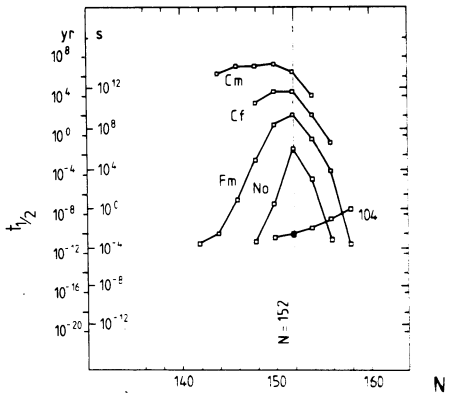

Fig. 10. Spontaneous fission halflife systematics for even-even nuclei.

This strange behaviour gave rise to discussions, whether the spontaneous fission activities observed in irradiations of targets near Pb with beams of ^{50}Ti and heavier might belong to actinide isomers, formed in transfer reactions (Viola, 1980).

We irradiated ^{208}Pb targets with ^{50}Ti of (4.75 - 5.15) MeV/u. At the lowest energies the 1n channel was identified by observation of the well known α-decay of ^{257}104, which also was found in correlations to decays of ^{253}No. With increasing projectile energy the expected ms spontaneous fission activity, assigned to ^{256}104, appeared. The width of the excitation function is about 10 MeV (Fig. 11), so we can exclude that this spontaneous fission activity originates from a transfer. Another proof is the agreement of our measured cross section to that given by Oganessian, which is about 6 nb in both cases. Similar arguments hold for α,xn channels. We do not observe any other decays in question for the isotope ^{256}104. Our halflife of $(8.1^{+1.1}_{-0.8})$ ms is in agreement to that measured by Oganessian (Fig. 12). At the highest energies we observed few spontaneous fission events with seconds halflife, which might belong to the isotope ^{255}104 and indicate the 3n channel.

This isotope also can be formed in the reaction ^{207}Pb (^{50}Ti, 2n) ^{255}104. We observed α-decays of ^{255}104 correlated to decays of ^{251}No and also spontaneous fission with corresponding halflife (Table 2).

TABLE 2 Isotopes from ^{40}Ar on Pb and Bi and ^{50}Ti on Pb irradiations. Error for decay energies ± 25 keV, halflife for 68 % probability.

Isotope	Energy/keV	$T_{1/2}$ / s
^{256}104	sf	$(8.1^{+1.3}_{-0.8}) \times 10^{-3}$
^{255}104	8 726,sf	$1.4^{+0.6}_{-0.3}$
^{247}Md	8 428	$2.9^{+1.7}_{-1.2}$
^{243}Fm	8 546	$0.18^{+0.08}_{-0.04}$
^{239}Cf	7 630	39^{+37}_{-12}

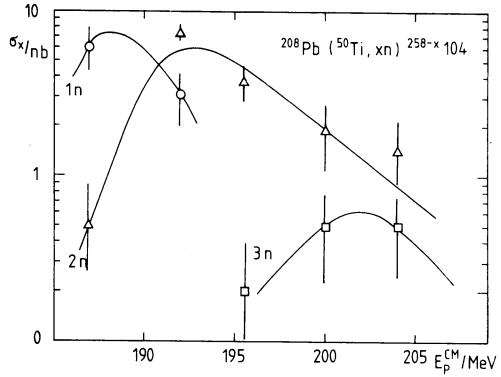

Fig. 11. Excitation function for ^{50}Ti on ^{208}Pb. Absolute error for cross section scale ($^{+100}_{-50}$) %, energy scale ± 2 MeV.

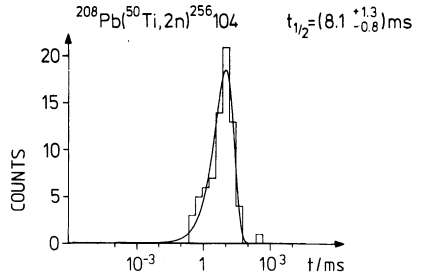

Fig. 12. Logarithmic distribution of time intervals between implantation and spontaneous fission of ^{256}104.

Fusion barrier. For the step from Ar to Ti the relative projectile charge and, hence, the Coulomb force of the nuclei interacting in the fusion process increases by 18 %. So it is an important question how much the fusion barrier is shifted to higher energies.

The fusion barrier can be extracted from the integral excitation function of evaporation residues formed via neutron evaporation (Schmidt, 1981), if certain assumptions are made. The cross section $\sigma_x(E)$ is obtained adding all cross sections of the various xn channels for a certain energy. Well below the fusion barrier it is mainly determined by barrier penetrability, well above by the neutron to fission width. The fusion barrier coincides approximately with the maximum of this excitation function.

From our data for ^{40}Ar on ^{208}Pb we obtain the excitation function, Fig. 13. The maximum is at (160±3) MeV. The energy can be converted to an effective Coulomb nucleon radius r_o^{eff} by use of the Coulomb law

$$r_o^{eff} = \frac{Z_p Z_t e^2}{E(A_p^{1/3}+A_t^{1/3})} \qquad (2)$$

Z_p and Z_t are the nuclear charge numbers of projectile and target, respectively, A_p and A_t are the corresponding mass numbers, e is the elemental charge, and E the projectile energy in the center of mass system. We obtain r_o^{eff} = (1.42±0.02) fm compared to the value of (1.44±0.01) fm obtained by Oganessian (1974) and also by Schulte (1981) from compound fission measurements. From the data of Schulte we obtain a fusion cross section of 50 mb corresponding to the maximum of the xn-excitation function.

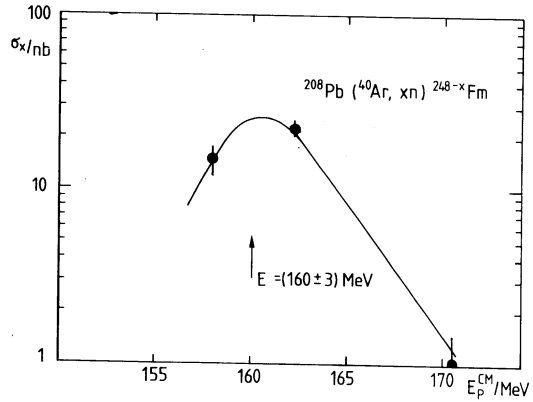

Fig. 13. Excitation function for ^{40}Ar on ^{208}Pb, for each energy the cross sections of all observed isotopes formed by neutron evaporation are added. Absolute error for cross section scale ($^{+100}_{-50}$) %, energy ± 2 MeV.

The integral xn excitation function for ^{50}Ti on ^{208}Pb is shown in Fig. 14 with maximum at (191±3) MeV or r_o^{eff} = (1.42±0.02) fm. A change of r_o^{eff} is not observed.

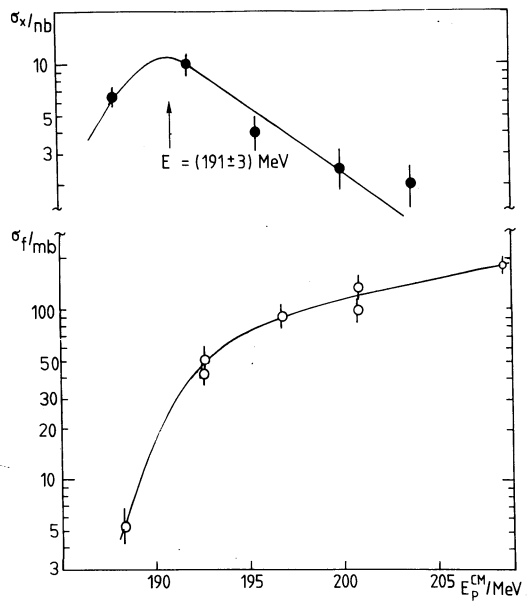

Fig. 14. Excitation function for ^{50}Ti on ^{208}Pb;
Upper curve : Evaporation residue cross section, taken from Fig. 11;
Lower curve : Fusion cross section from fusion fission.

From the symmetric mass component, also measured in our experiment, we get the excitation function for the total fusion cross section, Fig. 14. As the measured mass distribution cannot be assigned unambiguously to the various types of nuclear interactions, we put a comparatively narrow window on the symmetric peak. Consequently, our fusion cross sections may be underestimated by a factor of two. The maximum of the evaporation residue cross section corresponds to a fusion cross section of 30 mb, similar to that for ^{40}Ar on ^{208}Pb.

^{50}Ti and ^{54}Cr on Bi Irradiations, Element 107

Element 105 isotopes, daughter decays of 107. In irradiations of ^{209}Bi with ^{50}Ti we expect the formation of ^{257,258}105. The isotope ^{257}105 is of special interest : In irradiations of ^{54}Cr on ^{209}Bi to produce element 107, Oganessian (1976) observed two spontaneous fission activities. One with a halflife of (1 - 2) ms was assigned to ^{261}107, the other one with 5 s was explained by an unobserved α-decay of ^{261}107 leading to ^{257}105, which was regarded to undergo spontaneous fission with the corresponding halflife. From the relative intensities of observed spontaneous fission events in both cases, for ^{261}107 as well as for ^{257}105 strong α-decay branches were postulated.

We irradiated ^{209}Bi with ^{50}Ti beams between 4.65 MeV/u and 4.95 MeV/u with an integral ion dose of about 10^{16} per energy. The 2n channel was observed at 4.85 MeV/u and 4.95 MeV/u by decay chains from ^{257}105 ending in the sequence ^{249}Md-^{245}Es. Due to the 50 % detector efficiency, most of them are incomplete. At 4.95 MeV/u we found the decay chain of Fig. 15, in which decays of 8940 keV and 8750 keV are correlated to the known transition of ^{249}Md. The statistical error probability of this chain is less than 10^{-9}. So we can assign the decays to the isotopes ^{257}105 and ^{253}Lr. This chain represents the decay pattern of a single implanted nucleus of ^{257}105, therefore, we have to consider that the given decay energies and time distances straggle around the exact values of α-decay energies and halflives.

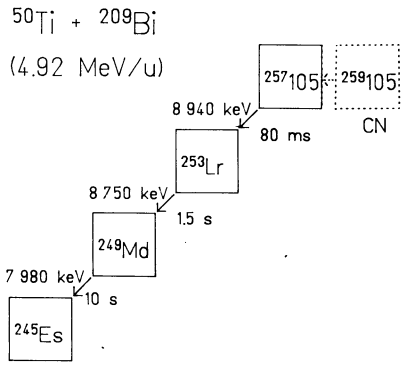

Fig. 15. α-decay chain of single implanted nucleus of ^{257}105, observed in ^{50}Ti on ^{209}Bi irradiation (2n).

At 4.75 MeV/u we observed decay chains, two examples of which are shown in Fig. 16. For the odd-odd nuclei α-decay as well as electron capture is expected. The electron capture decay of ^{258}105 would lead to the spontaneous fissioning ^{258}104.

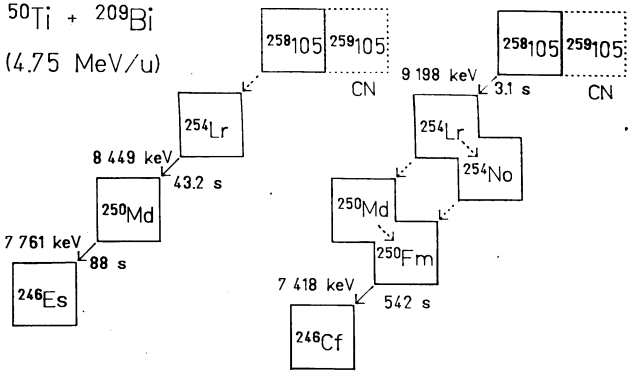

Fig. 16. Decay chains of two implanted nuclei of ^{258}105 observed in ^{50}Ti on ^{209}Bi irradiations (1n).

The decay characteristics of the Lr and 105 isotopes from the 1n channel are up to our present state of data evaluation for ^{258}105 two decay energies, 9189 keV and 9073 keV and (3.3±0.7) s halflife, for ^{254}Lr the decay energy 8459 keV, and the halflife (16±4) s. The decay chains end in known transitions of ^{254}No, ^{250}Fm, ^{250}Md.

The errors of the decay energies are ± 35 keV. Halflives may be corrected in the course of our further data evaluation, as up to now only the most significant events have been analyzed, for instance those correlated to daughter decays or with short time distances to the evaporation residues.

We observed 12 spontaneous fission events with a halflife of $(3.9^{+1.6}_{-0.9})$ s one at 4.65 MeV/u, 7 at 4.75 MeV/u, 3 at 4.85 MeV/u, and one at 4.95 MeV/u. The peak cross section is about 0.7 nb in good agreement to Oganessian, who measured 0.8 nb.

TABLE 3 Decays observed in ^{50}Ti and ^{54}Cr on ^{209}Bi irradiations. The error for decay energies is ± 25 keV. The halflife is for 60 % probability.

Isotope	Energy/keV	$T_{1/2}$ / s	
^{262}107	10 376	$(4.7^{+2.3}_{-1.6})$ x 10^{-3}	
^{258}105	9 189 9 073	3.3±0.7	Preliminary Data
^{257}105	9 161 9 049 8 946	0.9±0.3	
^{254}Lr	8 459	16 ±4	
^{253}Lr	8 824 8 743	2.6±1	
Spontaneous fission			
^{50}Ti+^{209}Bi	12 events	$3.9^{+1.6}_{-0.9}$	
^{54}Cr+^{209}Bi	1 event	3^{+6}_{-2}	

Element 107. Intention of our experiment was to identify element 107 by genetic relationships and to find its α-decay in correlation to decays of 105 and 103 observed in the ^{50}Ti on ^{209}Bi bombardments, and possibly down to transitions of ^{250}Fm or ^{250}Md. From our previous experimental results we calculated an effective radius of (1.42±0.02) fm for the maximum of the excitation function corresponding to 4.85 MeV/u and 4.95 MeV/u.

Figure 17 shows a plot of position and time correlations of evaporation residues, characterized by an energy signal exceeding 17 MeV which we calculated for our setup and a time-of-flight signal versus daughter decays, characterized by an energy between 7 MeV and 14 MeV, and an anticoincidence to the time-of-flight detector. Correlation time is limited to 200 ms, position

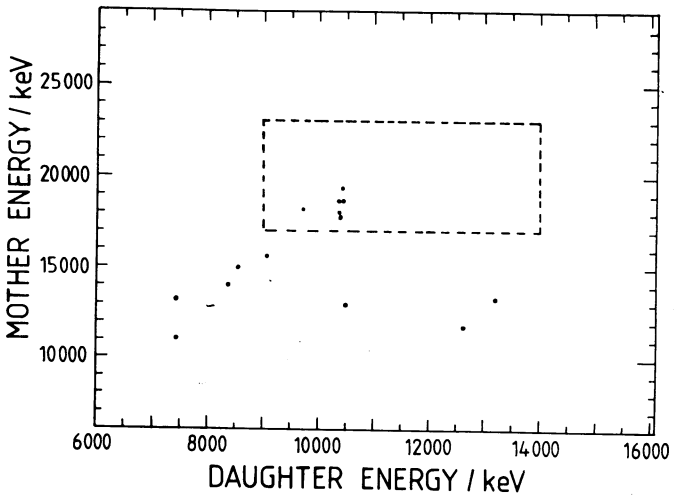

Fig. 17. Correlations observed in ^{54}Cr on ^{209}Bi irradiations. Maximum correlation time 200 ms, position window ± 0.5 mm. The two-dimensional energy window includes the expected energy range for evaporation residues and α-decays of element 107. Integral ion dose 1.2 x 10^{17}.

to ± 0.5 mm. In this two-dimensional window we find five events with a sharp energy of 10.4 MeV and one event of 9.7 MeV well separated from a small background.

Mother events with energy signals below 17 MeV are Bi-like recoils Their average energy is (14±1) MeV and 18 % below the average value for the evaporation residues,which is 17 MeV. As time-of-flight is similar, the energy difference corresponds to the mass difference between Bi and the compound nucleus which is 21 %.

Time distances between implantation and decay for the 10.4 MeV events range from (1 - 13) ms, that of the 9.7 MeV event is 165 ms. The halflife of the short lived events is 4.7 ms (Fig. 18). The time interval of the 9.7 MeV event does not fit to their time distribution.

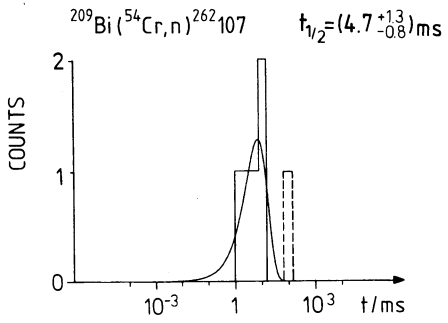

Fig. 18. Time correlation for the events found in the two-dimensional window of Fig. 17.

One of the observed events is correlated to a decay chain ending in ^{254}Lr, two of them end in ^{250}Fm decay, and one ends in ^{250}Md. An example of a complete decay chain is shown in Fig. 19.

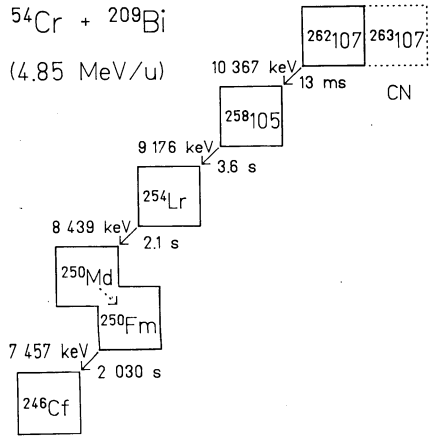

Fig. 19. α-decay chain of a single nucleus of element 107.

The results of the irradiations are collected in Table 3. The α-decay energy of ^{262}107 has been measured to (10.376±35) keV. One of the observed decays connected to a correlation chain has an energy of (9704±50) keV and its most probable halflife differs considerably from that of the other decays. In this case we have to consider that the evaporation residues are implanted into the detector close to its surface, hence the possibility that not the full energy of an α-decay is measured, cannot be excluded. For our case the probability for a decay with degraded energy between 9 and 10 MeV is less than 5 %.

At 4.85 MeV one spontaneous fission with a time distance of 4.3 s to the implantation of the evaporation residue was observed.

The cross section calculated from our counting rate is of the order 0.2 nb, the integral dose of irradiation was 1.2 x 10^{17} particles.

DISCUSSION

The identification of the isotopes ^{255},^{256}104 by their spontaneous fission and their assignment (Oganessian, 1975) is supported by our results. The change in spontaneous fission halflife systematics when leaving the actinide region, as found by Oganessian and calculated by Randrup (1973) could be confirmed.

The assignment of the spontaneous fission observed in the ^{50}Ti on ^{209}Bi irradiations is not facilitated by our experimental results, as we have to take into account also the 1n channel as possible source for this activity.

Spontaneous fission halflife of odd nuclei is hindered by a factor of about 10^3 for each odd nucleon (Swiatecki, 1955). From the 8.1 ms halflife of ^{256}104, we expect a partial spontaneous fission halflife of more than 10^3 s for the odd-odd ^{258}105. From this point of view this isotope will not undergo spontaneous fission itself. The predicted β halflife is 16 s (Kolesnikov, 1975), so it may have a strong electron capture branch leading to the spontaneous fissioning ^{258}104, which has a halflife of tens of milliseconds. Consquently, its fission would be observed with the halflife of ^{258}105.

The nuclide ^{257}105 is expected to undergo spontaneous fission. Our opinion is, that the spontaneous fission activity in ^{50}Ti on ^{209}Bi irradiation could originate as well from the 1n as from the 2n channel as we observed it together with α-decay from ^{258}105 as well as from ^{257}105.

In this experiment the first identification of element 107 by genetic relationship is performed. Spontaneous fission of the identified odd-odd isotope ^{262}107 is not expected, electron capture leading to ^{262}106 which is supposed to undergo spontaneous fission can be excluded from β halflife predictions.

The one spontaneous fission event is likely to belong to a daughter decay, as the lifetime agrees with that measured in the ^{50}Ti in ^{209}Bi irradiations.

The odd mass nucleus, ^{261}107 which might be formed by 2 neutron evaporation could not be found, possibly due to the low excitation energy of the compound systems produced.

Our experimental results show that the use of targets near the double magic ^{208}Pb makes it possible to form cold compound nuclei close to fusion barrier even for the heaviest systems known up to now. This is advantageous especially for the production of nuclei with Z ≥ 105, as shown in Fig. 20. Here, the maximum cross sections obtained experimentally for the production of the heaviest elements are plotted for the combinations actinide target and light projectile, Pb-like target and heavy beam, and, for comparison, also for α induced reactions.

The effective Coulomb radius of (1.42±0.02) fm describes the position of the maximum of the excitation function for all investigated reactions, so we can hope to produce even heavier compound systems with low excitation energies.

The nuclei formed in the chosen target projectile combinations need no extra energy above the Coulomb barrier to undergo fusion. So we have a new hope, to reach the island of superheavy nuclei by cold fusion of ^{48}Ca and ^{248}Cm.

It is expected that fusion of very heavy systems is limited by the strong Coulomb forces. This process can be characterized by the scaling factor $(Z^2/A)_{eff}$ (Swiatecki, 1980). From the presented results as well as from the data of Schmidt (1981) no enhancement of the barrier, e.g. no reduction of r_o^{eff} is observed even for Z^2/A_{eff} values exceeding that for ^{48}Ca on ^{248}Cm (Fig. 21). With an effective Coulomb radius of 1.40 fm the excitation energy of the compound system at the fusion barrier has the unexpected low value of 28 MeV. As reasonable cross sections can be expected also below the barrier (Schmidt, 1981), there is some hope that the formation of a superheavy evaporation residue is possible by evaporation of one neutron with (4.7 - 4.9) MeV/u projectile energies.

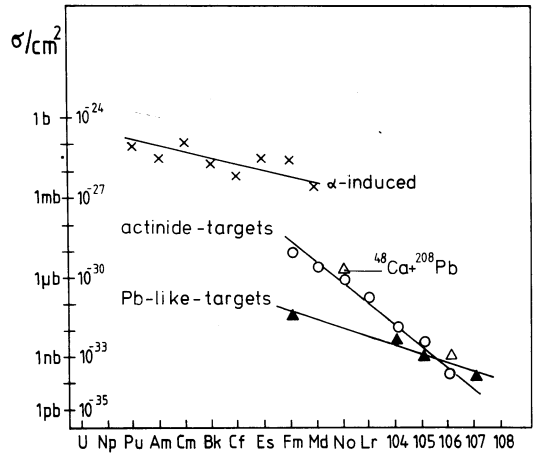

Fig. 20. Maximum cross sections for production of transuranium isotopes (Gmelin, 1974), black marked this work.

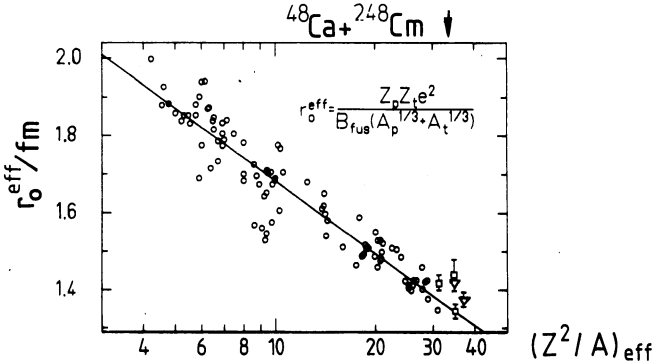

Fig. 21. Effective radius parameter in dependence of $(Z^2/A)_{eff}$. Circles Vaz (1980), triangles Schmidt (1981), squares this work.

ACKNOWLEDGEMENT

We are indebted to the UNILAC team, the crew preparing the ion sources for the enriched beams, the GSI target-laboratory, the experimental electronic department for their excellent collaboration, making these difficult experiments possible, to D. Hildenbrand and W. Schneider for their help to develop the large area time-of-flight detector.

REFERENCES

Faust, W., G. Münzenberg, S. Hofmann, W. Reisdorf, K.-H. Schmidt, P. Armbruster (1979). Nucl. Instr. Meth. 166, 397-405

Gäggeler, H., A.S. Iljinov, G.S. Popeko, W. Seidel, G.M. Ter-Akopian, S.P. Tretaykova (1979). Z. Phys. A289, 415-420

Gmelin, L. (1974). Gmelin Handbuch der Anorganischen Chemie 76, 60-97

Hofmann, S., W. Faust, G. Münzenberg, W. Reisdorf, P. Armbruster, K. Güttner, H. Ewald (1979). Z Phys. A291, 53-70

Hofmann, S., G. Münzenberg, F.P. Heßberger, W. Reisdorf, P. Armbruster, B. Thuma (1981a). Z. Phys. A299, 281-282

Hofmann, S., G. Münzenberg, W. Faust, F.P. Heßberger, W. Reisdorf, J.R.H. Schneider, P. Armbruster, K. Güttner, B. Thuma (1981b). Proceedings on the International Conference on Nuclei far from Stability, Helsingør, Denmark

Kolesnikov, N.N., A.G. Demin (1975). Communication JINR PG-9421, Dubna

Lederer, C.M., V. Shirley ed. (1978). Table of Isotopes, J. Wiley & Sons Inc., New York

Münzenberg, G., W. Faust, S. Hofmann, P. Armbruster, K. Güttner, H. Ewald, (1979). Nucl. Instr. Meth. 161, 65-82

Münzenberg, G., W. Faust, F.P. Heßberger, S. Hofmann, W. Reisdorf, K.-H. Schmidt, W.F.W. Schneider, H.J. Schött, P. Armbruster, B. Thuma, H. Ewald, D. Vermeulen (1981a). Nucl. Instr. Meth. 186, 423-433

Münzenberg, G., S. Hofmann, W. Faust, F.P. Heßberger, W. Reisdorf, K.-H. Schmidt, T. Kitahara, P. Armbruster, K. Güttner, B. Thuma, D. Vermeulen (1981b). Z. Phys. A, in print

Münzenberg, G., S. Hofmann, F.P. Heßberger, W. Reisdorf, K.-H. Schmidt, W. Faust, P. Armbruster, K. Güttner, B. Thuma, D. Vermeulen, C.C. Sahm, (1981c). Proceedings on the International Conference of Nuclei far from Stability, Helsingør, Denmark

Münzenberg, G., S. Hofmann, F.P. Heßberger, W. Reisdorf, K.-H. Schmidt, J.R.H. Schneider, P. Armbruster, C.C. Sahm, B. Thuma (1981d). Z. Phys. A100, 107-108

Nitschke, J.M., R.E. Leber, M.J. Nurmia, A. Ghiorso (1979). Nucl. Phys. A313, 236-250

Oganessian, Yu.Ts., Yu.E. Penionzhkevich, K.A. Gavrilov, Kim De En (1974). JINR P7-7863, Dubna

Oganessian, Yu.Ts., A.S. Iljinov, A.G. Demin, S.P. Tretyakova (1975a). Nucl. Phys. A239, 353-364

Oganessian, Yu.Ts., A.G. Demin, A.S. Iljinov, S.P. Tretyakova, A.A. Pleve, Yu.E. Penionzhkevich, M.P. Iwanov, Yu.P. Tretyakov (1975b). Nucl. Phys. A239, 157-171

Oganessian, Yu.Ts., A.G. Demin, N.A. Danilov, G.N. Flerov, M.P. Ivanov, A.S. Iljinov, N.N. Kolesnikov, B.N. Markov, V.M. Plotko, S.P. Tretyakova (1976). Nucl. Phys. A273, 305-522

Randrup, J., C.F. Tsang, P. Möller, S.G. Nilsson, S.E. Larsson (1973). Nucl. Phys. A217, 221-237

Sahm, C.C., H. Schulte, D. Vermeulen, J. Keller, H.G. Clerc, K.-H. Schmidt, F.P. Heßberger, G. Münzenberg (1980). Z. Phys. A297, 241-245

Schmidt, K.-H., W. Faust, G. Münzenberg, H.-G. Clerc, W. Lang, K. Pielenz, D. Vermeulen, H. Wohlfarth, H. Ewald, K. Güttner (1979). Nucl. Phys. A318, 253-268

Schmidt, K.-H., P. Armbruster, F.P. Heßberger, G. Münzenberg, W. Reisdorf, C.C. Sahm, D. Vermeulen, H.-G. Clerc, J. Keller, H. Schulte (1981). Z. Phys. A301, 21-28

Schulte, H. (1981). Diploma work, Darmstadt

Swiatecki, W.J. (1955). Phys. Rev. 100, 937-938

Swiatecki, W.J. (1980). Preprint LBL/10911, Berkeley

Vermeulen, D., H.-G. Clerc, W. Lang, K.-H. Schmidt, G. Münzenberg (1980). Z. Phys. A294, 149-151

Viola jr., V.E., A.C. Mignerey, H. Breuer, K.L. Wolf, G.L. Glagota, W.W. Wilcke, W.K. Schröder, J.R. Huizenga, D. Hilscher, J.R. Birkelund (1980). Phys. Rev. C22, 122-127

Vaz, L.C., J.M. Alexander, G.R. Satchler (1980). Preprint